

See discussions, stats, and author profiles for this publication at: <https://www.researchgate.net/publication/230868585>

High Mobility, Air Stable, Organic Single Crystal Transistors of an n-Type Diperylene Bisimide

ARTICLE *in* ADVANCED MATERIALS · MAY 2012

Impact Factor: 17.49 · DOI: 10.1002/adma.201104987

CITATIONS

68

READS

73

14 AUTHORS, INCLUDING:



Aifeng Lv

Chinese Academy of Sciences

11 PUBLICATIONS 202 CITATIONS

SEE PROFILE

Sreenivasa Reddy Puniredd

Agency for Science, Technology and Resear...

48 PUBLICATIONS 770 CITATIONS

SEE PROFILE



Huanli Dong

Chinese Academy of Sciences

108 PUBLICATIONS 2,618 CITATIONS

SEE PROFILE



Yan Li

Dalian University of Technology

675 PUBLICATIONS 9,479 CITATIONS

SEE PROFILE

High Mobility, Air Stable, Organic Single Crystal Transistors of an n-Type Diperylene Bisimide

Aifeng Lv, Sreenivasa R. Puniredd, Jiahui Zhang, Zhibo Li,* Hongfei Zhu, Wei Jiang, Huanli Dong, Yudong He, Lang Jiang, Yan Li, Wojciech Pisula, Qing Meng, Wenping Hu,* and Zhaohui Wang*

The design and synthesis of organic semiconductors with high mobility and stability, especially n-type organic semiconductors, are essential for the development of organic circuits and organic electronics.^[1] Compared to p-type organic semiconductors, the development of n-type organic semiconductors has lagged because of their high sensitivity to ambient conditions.^[2] Recently, some impressive progress has been made by functionalization of (hetero-)acenes, thiophenes, and arylenes with electron-deficient constituents.^[3–5] However, the development of air-stable, high mobility, n-type organic semiconductors for organic electronics is still highly emergent.

The mobility of organic semiconductors depends on the efficiency of charge transport from one molecule to another. Hence, some organic semiconductors with dense molecule packing always give high mobility.^[6] As to the stability of organic compounds, it is believed that the highest occupied molecular orbital (HOMO) of p-type organic semiconductors should be more negative than –5.0 eV, e.g., locating at –5.0 to –6.0 eV, and the lowest unoccupied molecular orbitals (LUMO) of n-type organic semiconductors are best located between –4.0 and –4.5 eV, for anti-oxidation in air.^[2,7] We have acknowledged these requirements and believe that perylene bisimides (PBIs) will fit as candidates because of their reasonable electron acceptor ability,^[8] and have been focusing on the expansion of the chemistry of perylene bisimides (PBIs) by a combination of Ullmann coupling and C–H transformation for some time, and have developed a facile strategy to synthesize fully conjugated, triply linked, diperylene bisimides,^[8] conferring the expanded

conjugated molecules with decent promising electrical properties over their synthetic precursor.^[9] Here, we report the synthesis of a novel n-type organic semiconductor, namely, tetrachlorinated diperylene bisimide (C12-4ClDiPBI, **Scheme 1**), by two simple steps. The facile synthesis makes it possible to scale up to kilogram levels. It is found that the LUMO level of C12-4ClDiPBI is around –4.22 eV, which makes C12-4ClDiPBI one of the most electron deficient n-type organic semiconductors. Single crystals of C12-4ClDiPBI are grown by a solution process, and transistors based on single crystals suggest that the electron mobility of C12-4ClDiPBI is as high as 4.65 cm² V^{–1} s^{–1}. Moreover, all devices exhibit excellent environmental stability. No obvious degradation is observed after the devices are kept in air for over one and half months. These characteristics imply a bright future of the n-type compound in cost-effective organic transistor circuits.

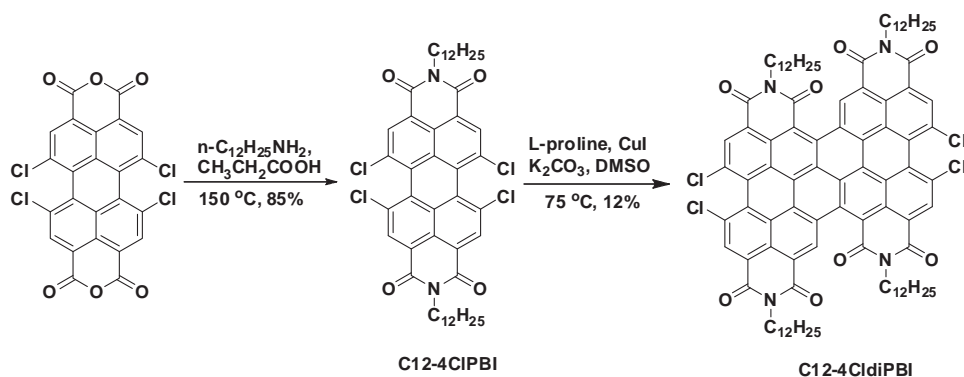
The design of the compound takes the following aspects into consideration: i) the expansion of the π -conjugated aromatic system is expected to enhance the stacking of molecules and thus facilitates electron transport,^[10] ii) four alkyl groups are integrated to the parent molecular framework, which will substantially improve the material's solubility and processability, and iii) additional tetra-chloro-constituents are expected to further lower the LUMO energy level of the compounds to enhance their ambient stability. The synthesis of C12-4ClDiPBI following optimized reaction conditions can be depicted by Scheme 1.^[8a,11] The homocoupling of C12-4ClPBI proceeded in DMSO at 75 °C with CuI as the reagent, L-proline as the ligand, and K₂CO₃ as the base in a moderate yield while the crude product could be purified easily by silica gel column chromatography and further characterized by NMR spectroscopy and matrix-assisted laser desorption–ionization time-of-flight mass spectrometry (MALDI-TOF MS). Due to the facile two-step synthetic route, the synthesis of C12-4ClPBI is easily scaled up to kilogram levels.

Attractively, C12-4ClDiPBI shows excellent solubility in common organic solvents such as chloroform, toluene, and chlorobenzene (>20 mg mL^{–1}) at room temperature, indicating its great potential for solution processed organic devices and circuits. The UV/vis absorption spectrum of C12-4ClDiPBI is shown in **Figure 1A**. The compound showed a wide absorption ranging from the UV-vis to NIR. The longest absorption wavelength is at around 690 nm, indicating that the optical energy bandgap of C12-4ClDiPBI is at ~1.8 eV. The wide absorption and narrow energy bandgap of C12-4ClDiPBI also suggests its

A. Lv, J. Zhang, Prof. Z. Li, Dr. H. Zhu, Dr. W. Jiang,
Dr. H. Dong, Y. He, Dr. L. Jiang, Dr. Y. Li, Dr. Q. Meng,
Prof. W. Hu, Prof. Z. Wang
Beijing National Laboratory for Molecular Sciences
Key Laboratory of Organic Solids
Institute of Chemistry
Chinese Academy of Sciences
Beijing 100190, P. R. China
E-mail: zbli@iccas.ac.cn; huwp@iccas.ac.cn; wangzhaohui@iccas.ac.cn
A. Lv, J. Zhang, Y. He
Graduate University of Chinese Academy of Sciences
Beijing 100039, P. R. China
Dr. S. R. Puniredd, Dr. W. Pisula
Max Planck Institute for Polymer Research
Ackermannweg 10, 55118 Mainz, Germany



DOI: 10.1002/adma.201104987



Scheme 1. Synthesis of contorted diperylene bisimides.

possible application in photoresponsive devices, such as photo-voltaic devices, photodetectors, and phototransistors.^[7]

The cyclic voltammogram of C12-4CldiPBI in CH_2Cl_2 is shown Figure 1B. It displays two distinct reversible and two quasireversible reduction peaks. The corresponding half-wave reduction potentials (vs Fc/Fc^+) of C12-4CldiPBI are summarized in Table 1. The first reduction potential of C12-4CldiPBI reaches -0.58 V. Given the energy level of Fc/Fc^+ is -4.8 eV in vacuum, the LUMO level of C12-4CldiPBI is estimated to be -4.22 eV (energy diagram is shown in Figure 1C), indicating the possible high stability of this compound.^[7] Moreover, TGA

measurements prove that the temperature for 5% weight loss is up to 389.5 °C (Figure 1D), indicating the excellent thermal stability of C12-4CldiPBI, which is also important for the practical application of the compounds into devices and circuits.

Single crystals of C12-4CldiPBI are grown by a solution process in order to better understand the properties of the compound because in a crystal there are no grain boundaries, and few traps and defects, which provides the most powerful tool to guide the structure–property insight of organic semiconductors.^[12] Through a solvent vapor diffusion strategy, micro and nanometer-sized ribbons of C12-4CldiPBI are

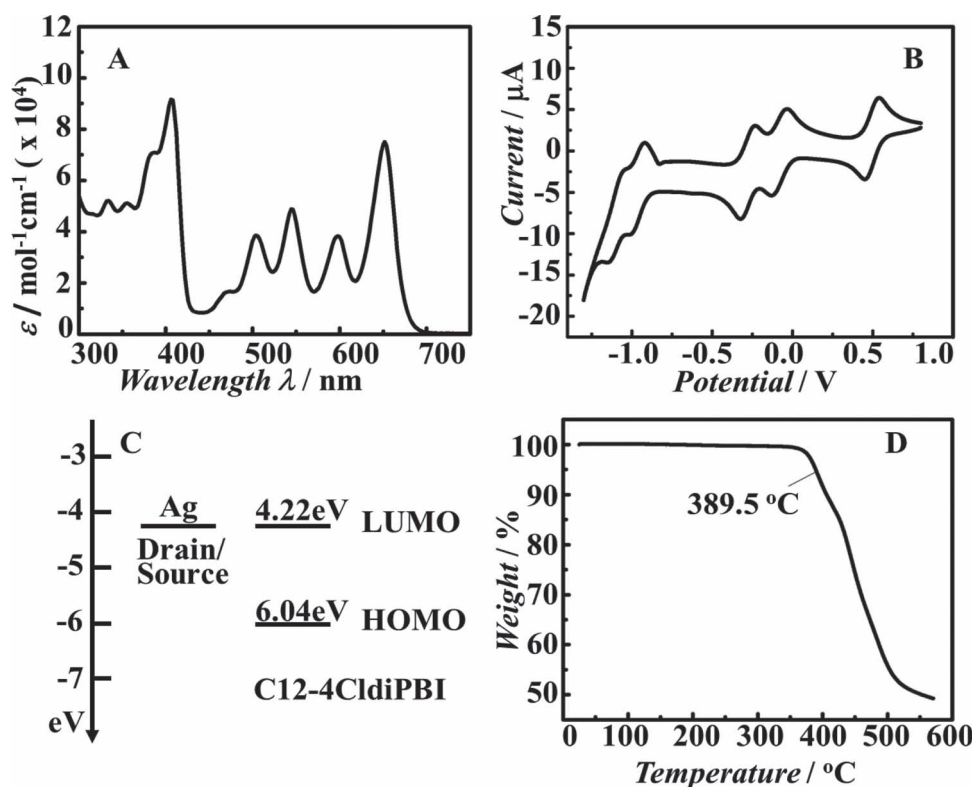


Figure 1. A) UV-Vis absorption spectrum and B) cyclic voltammogram of C12-4CldiPBI in CH_2Cl_2 . The plot in C) shows the energy level diagram between C12-4CldiPBI and Ag electrodes. D) TGA plot of C12-4CldiPBI.

Table 1. Redox potentials (in V vs Fc/Fc⁺)^{a)}

Compound	E_{1r}	E_{2r}	E_{3r}	E_{4r}
C12-4ClPBI	−0.86	−1.05	—	—
C12-4ClDiPBI	−0.58	−0.77	−1.46	−1.60

^{a)}Half-wave potentials. The data have been calculated to the reference of Fc/Fc⁺. The concentration is 0.5×10^{-3} M. Scan rate is 0.2 V s^{-1} and the electrolyte is 0.1 M TBAPF₆. The plot includes the signal of the ferrocene (Fc) standard with its oxidation potential at 0.49 V .

obtained from toluene/methanol solution. As shown in the scanning electron microscopy (SEM) image in **Figure 2A** (and **Figure S3**, Supporting Information), the products are highly

regular belts ranging from several hundreds of nanometers to micrometers in length. A powder X-ray diffraction (XRD) pattern of the belts is shown in **Figure 2B**. The baseline is relatively straight and the diffraction peaks are very sharp, indicating the high quality of the C12-4ClDiPBI single crystals. A transmission electron microscopy (TEM) image of an individual nanoribbon and its corresponding selected area electron diffraction (SAED) pattern are shown in **Figure 2C** and **D**. The SAED patterns of the ribbon at different places showed identical patterns, indicating the whole ribbon is a single crystal. The thicknesses of the ribbons were characterized by atomic force microscopy (AFM), suggesting the thickness of ribbons varied from tens of nanometers to several micrometers.

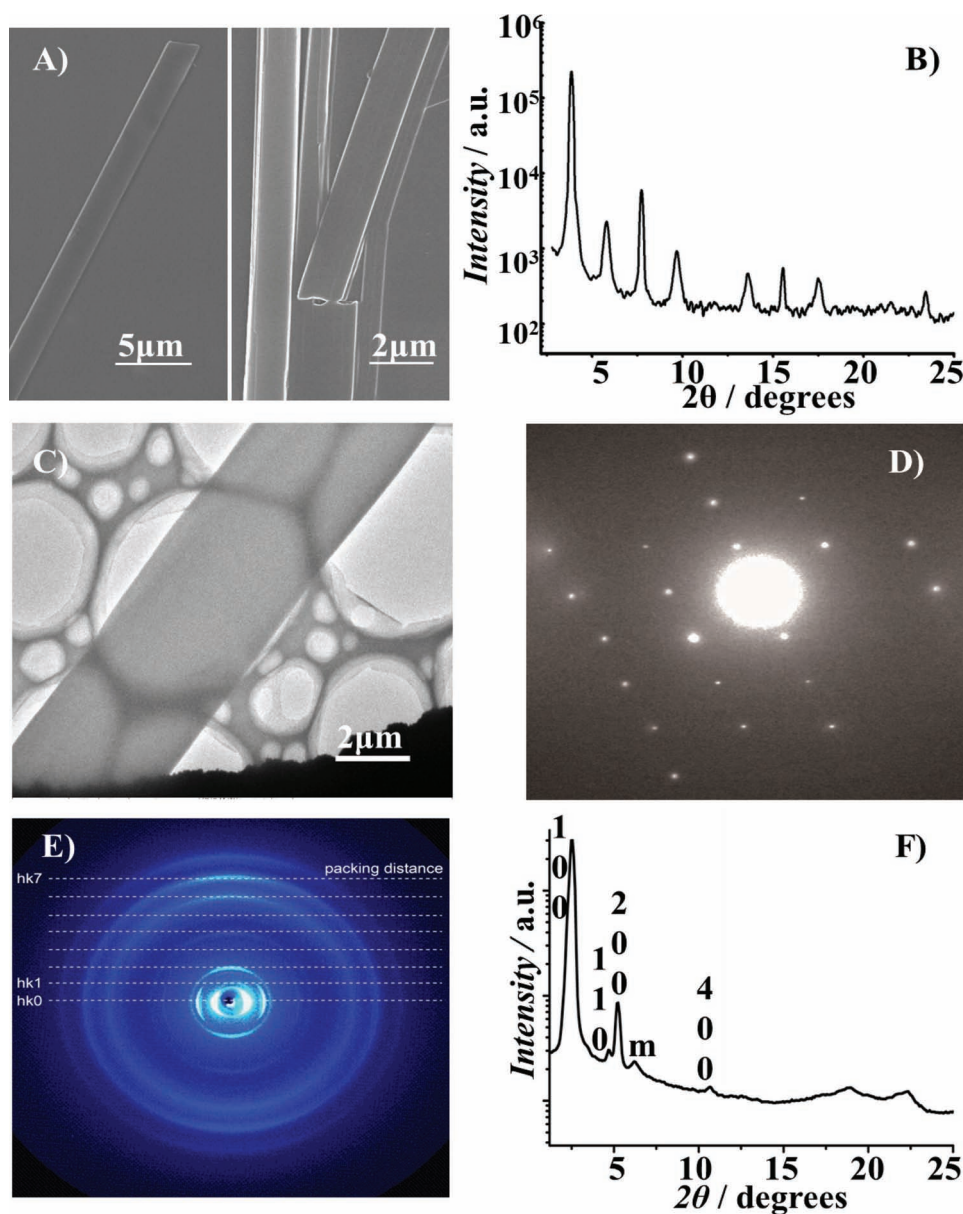


Figure 2. A) SEM image of micro/nanobelts. B) Powder XRD pattern of C12-4ClDiPBI micro/nanobelts. C) TEM image of a micro/nanobelt and D) its corresponding SAED pattern. E) 2D WAXS pattern (scattering lines due to helical organization assigned by Miller indices) and F) the equatorial integration (reflections are assigned by Miller indices according to a hexagonal unit cell; m = meridional reflection) of C12-4ClDiPBI.

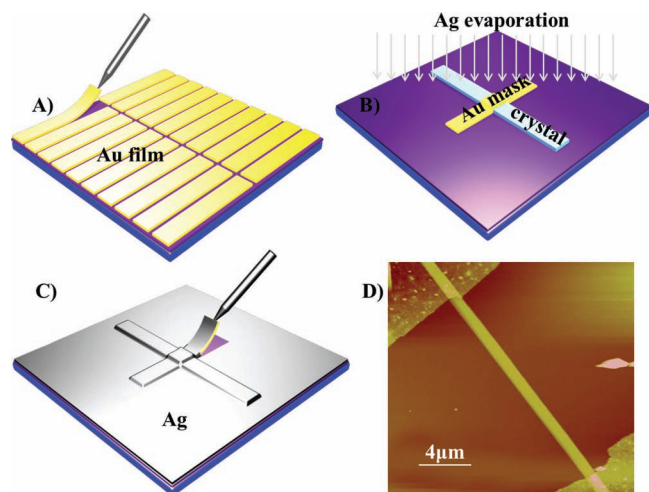


Figure 3. A–C) Scheme of the device fabrication process. D) AFM image of a finished transistor based on an individual nanoribbon.

The molecular organization of C12-4CldiPBI is further examined by two-dimensional wide-angle X-ray scattering (2D WAXS) on extruded fibers as shown in Figure 2E and F. The scattering intensities on the equatorial $hk0$ line of the pattern are related to a hexagonal intercolumnar arrangement with $a_{\text{hex}} = 3.80$ nm as the unit cell parameter. Moreover, each of the reflections can be assigned to specific scattering lines which are evenly spaced from each other. The position of the middle-angle meridional reflection on the $hk1$ line is related to a period of 2.8 nm along the columnar axis, while the $hk7$ line corresponds to the packing distance of 0.4 nm between the building blocks. The ratio of both distances indicates that every 7th molecule is in the same lateral position. This is also the helix length along the columnar stack in which the C2 symmetric C12-4CldiPBI molecules are rotated by ca. 51.4° to each other so that the 7th disk is finally rotated by a full 360° . This structure allows the peripheral hindrance at the core proximity to be overcome.

Field-effect transistors based on individual micro- or nanoribbons of C12-4CldiPBI are fabricated with octadecyltrichlorosilane (OTS)-treated SiO_2/Si substrates as an insulator/gate electrode. Ag is selected as the material for the source and drain electrodes in order to align the work function of the electrodes (4.2 eV) with the LUMO level of C12-4CldiPBI (4.22 eV). This good energy level alignment provides the pre-requirement for efficient charge injection from the source electrode into C12-4CldiPBI and charge collection from C12-4CldiPBI back to the drain electrode. A technique named “Au stripe mask” has been developed^[13] to fabricate transistors based on the small crystals of C12-4CldiPBI. The fabrication process is depicted by Figure 3. First, a Au film with a thickness of around 100 nm is deposited

on a Si wafer by thermal evaporation. The film is then cut into Au strips by the tip of a mechanical probe with widths from a few micrometers to tens of micrometers and lengths of around ~ 150 mm. A strip is then peeled off from the Si substrate by the mechanical probe and transferred onto the single crystal ribbon of C12-4CldiPBI to serve as the mask for the next Ag deposition. Afterwards, a 60 nm Ag film is deposited on the substrate as source and drain electrodes. Finally, the Au mask strip is peeled off from the micro/nanoribbons and a device based on an individual single crystal ribbon of C12-4CldiPBI is available. A representative example device is shown in Figure 3D.

The performance of the transistors is characterized by a Keithley 4200-SCS semiconductor parameter analyzer and a Micromanipulator 6150 probe station in a clean and shielded box. All characterizations of the n-type organic transistors are performed in air to examine its environmental stability. Representative transfer and output characteristics of the transistors are shown in Figure 4A and B. The device exhibits excellent n-type transistor behavior with negligible hysteresis indicating the high quality of the interface between the organic crystal and the gate insulator. The lack of saturation at high drain voltages is probably attributable to the solvent doping.^[14] It is also noticed that devices with channel length ranging from 15 to $30\ \mu\text{m}$ show better performance. Nearly 50 transistors with a channel length located in this range have been measured. The mobility distribution is shown in Figure 4C. All devices give an electron mobility over $1.0\ \text{cm}^2\ \text{V}^{-1}\ \text{s}^{-1}$ with the highest mobility of $4.65\ \text{cm}^2\ \text{V}^{-1}\ \text{s}^{-1}$, which is much higher than that of thin film transistors (see Supporting Information). Finally, it should be addressed that the transistors of C12-4CldiPBI exhibit excellent air stability. No obvious degradation is observed even keeping the devices in air over one and half months (Figure 4D).

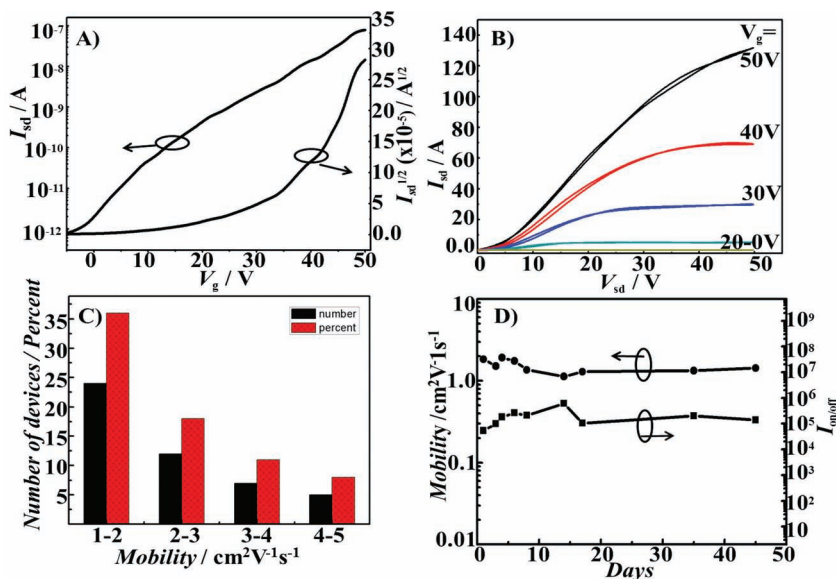


Figure 4. A) Typical transfer and B) output curve of organic single-crystal field effect transistors (SCFETs) based on a micro/nanobelt with Ag as the electrodes. C) The statistics of the 49 devices: the distribution/percent of the mobility. D) Air-stability test on one of the best SCFETs over a period of nearly 50 days.

In conclusion, a new n-type organic semiconductor, C12-4CldiPBI, is synthesized by a simple and facile route. The LUMO level of C12-4CldiPBI is down to -4.22 eV, which makes it one of the most electron deficient n-type organic semiconductors, and is well aligned to the work function of Ag electrodes (4.2 eV). Single crystal ribbons of C12-4CldiPBI are grown facilely by a solvent vapor diffusion strategy. Organic field-effect transistors based on individual ribbons are fabricated by a new technique named "Au stripe mask" method. Around 50 devices with a channel length of $15\text{--}30\text{ }\mu\text{m}$ are examined. The device exhibits excellent n-type transistor behavior with negligible hysteresis. All devices give an electron mobility over $1.0\text{ cm}^2\text{ V}^{-1}\text{ s}^{-1}$ with the highest mobility of $4.65\text{ cm}^2\text{ V}^{-1}\text{ s}^{-1}$. Moreover, the devices exhibit excellent air stability. No obvious degradation is observed even keeping the devices in air for over one and half months. The facile synthesis of the compound, the high mobility, and excellent air stability of the n-type compound suggest a bright future for C12-4CldiPBI in cost-effective organic electronics.

Experimental Section

The substrates used here were successively cleaned with pure water, piranha solution ($\text{H}_2\text{SO}_4/\text{H}_2\text{O}_2 = 7:3$), pure water, pure isopropyl alcohol, and finally blown dry with high-purity nitrogen gas. Treatment of the Si/SiO₂ wafers with OTS was carried out by the vapor-deposition method. The clean wafers were dried under vacuum at 90°C for 0.5 h in order to eliminate the influence of moisture. When the temperature decreased to 70°C , a small drop of OTS was placed around the wafers. Subsequently, this system was heated to 120°C and maintained for 2 h under vacuum.

Firstly, 1 mg of C12-4CldiPBI was dissolved in 1 mL of toluene in a sample vial. Secondly, 1 mL of methanol was injected into a larger vial. Thirdly, the smaller sample vial was placed into the larger vial which was then sealed. After two or three days, the single crystal nanoribbons deposited from the solvent.

SEM images were obtained with a Hitachi S-4300 microscope (Japan). AFM was performed with a Nanoscopy IIIa (USA). TEM and SAED measurements were carried out using a JEOL-1011 (Japan). XRD was measured on a D/max2500 with a Cu K α source ($\lambda = 1.541\text{ \AA}$).

Acknowledgements

The authors acknowledge the financial support from National Natural Science Foundation of China (91027043, 20721061, 51033006, 51003107, 21190032), the China-Denmark Co-project, TRR61 (NSFC-DFG Transregio Project), the Ministry of Science and Technology of China (2010CB808400, 2011CB932300) and Chinese Academy of Sciences.

Received: December 31, 2011

Revised: March 3, 2012

Published online: April 13, 2012

- [1] a) Z. Bao, J. J. Locklin, *Organic field-effect transistors*, CRC Press, Boca Raton, FL **2007**; b) H. Klauk, *Organic Electronics: Materials, Manufacturing, and Applications*, Wiley-VCH, Weinheim, Germany **2006**; c) C. Wang, H. Dong, W. Hu, Y. Liu, D. Zhu, *Chem. Rev.* **2012**,

- 112, 10.1021/cr100380z.; c) Y. Wen, Y. Liu, Y. Guo, G. Yu, W. Hu, *Chem. Rev.* **2011**, 111, 3358; d) H. Dong, H. Zhu, Q. Meng, X. Gong, W. Hu, *Chem. Soc. Rev.* **2012**, 41, 1754.
- [2] a) C. R. Newman, C. D. Frisbie, D. A. da Silva Filho, J.-L. Brédas, P. C. Ewbank, K. R. Mann, *Chem. Mater.* **2004**, 16, 4436; b) L. Jiang, H. L. Dong, W. P. Hu, *J. Mater. Chem.* **2010**, 20, 4994; c) Y. G. Wen, Y. Q. Liu, *Adv. Mater.* **2010**, 22, 1331; d) J. E. Anthony, A. Facchetti, M. Heeney, S. R. Marder, X. Zhan, *Adv. Mater.* **2010**, 22, 3876.
- [3] a) H. E. Katz, A. J. Lovinger, J. Johnson, C. Kloc, T. Siegrist, W. Li, Y. Y. Lin, A. Dodabalapur, *Nature* **2000**, 404, 478; b) H. Yan, Z. Chen, Y. Zheng, C. Newman, J. R. Quinn, F. Dötz, M. Kastler, A. Facchetti, *Nature* **2009**, 457, 679.
- [4] a) R. Schmidt, M. M. Ling, J. H. Oh, M. Winkler, M. Könnemann, Z. Bao, F. Würthner, *Adv. Mater.* **2007**, 19, 3692; b) M. Gsänger, J. H. Oh, M. Könnemann, H. W. Höffken, A.-M. Krause, Z. Bao, F. Würthner, *Angew. Chem. Int. Ed.* **2010**, 49, 740; c) R. Schmidt, J. H. Oh, Y. S. Sun, M. Deppisch, A. M. Krause, K. Radacki, H. Braunschweig, M. Könnemann, P. Erk, Z. N. Bao, F. Würthner, *J. Am. Chem. Soc.* **2009**, 131, 6215; d) J. H. Oh, S.-L. Suraru, W.-Y. Lee, M. Könnemann, H. W. Höffken, C. Röger, R. Schmidt, Y. Chung, W.-C. Chen, F. Würthner, Z. Bao, *Adv. Funct. Mater.* **2010**, 20, 2148; e) W.-Y. Lee, J. H. Oh, S.-L. Suraru, W.-C. Chen, F. Würthner, Z. Bao, *Adv. Funct. Mater.* **2011**, 21, 4173.
- [5] a) X. Gao, C.-a. Di, Y. Hu, X. Yang, H. Fan, F. Zhang, Y. Liu, H. Li, D. Zhu, *J. Am. Chem. Soc.* **2010**, 132, 3697; b) Z. Liang, Q. Tang, J. Xu, Q. Miao, *Adv. Mater.* **2011**, 23, 1535; c) H. N. Tsao, D. M. Cho, I. Park, M. R. Hansen, A. Mavrinskiy, D. Y. Yoon, R. Graf, W. Pisula, H. W. Spiess, K. Müllen, *J. Am. Chem. Soc.* **2011**, 133, 2605.
- [6] a) H. Meng, F. P. Sun, M. B. Goldfinger, G. D. Jaycox, Z. G. Li, W. J. Marshall, G. S. Blackman, *J. Am. Chem. Soc.* **2005**, 127, 2406; b) H. Meng, F. P. Sun, M. B. Goldfinger, F. Gao, D. J. Londono, W. J. Marshall, G. S. Blackman, K. D. Dobbs, D. E. Keys, *J. Am. Chem. Soc.* **2006**, 128, 9304; c) L. Li, Q. Tang, H. Li, X. Yang, W. Hu, Y. Song, Z. Shuai, W. Xu, Y. Liu, D. Zhu, *Adv. Mater.* **2007**, 19, 2613.
- [7] H. Dong, C. Wang, W. Hu, *Chem. Commun.* **2010**, 46, 5211.
- [8] a) H. Qian, Z. Wang, W. Yue, D. Zhu, *J. Am. Chem. Soc.* **2007**, 129, 10664; b) H. Qian, F. Negri, C. Wang, Z. Wang, *J. Am. Chem. Soc.* **2008**, 130, 17970; c) Y. Zhen, C. Wang, Z. Wang, *Chem. Commun.* **2010**, 46, 1926; d) Y. Li, L. Tan, Z. Wang, H. Qian, Y. Shi, W. Hu, *Org. Lett.* **2008**, 10, 529; e) Y. Li, C. Li, W. Yue, W. Jiang, R. Kopecek, J. Qu, Z. Wang, *Org. Lett.* **2010**, 12, 2374.
- [9] a) Z. Chen, M. G. Debije, T. Debaerdemaeker, P. Osswald, F. Würthner, *ChemPhysChem* **2004**, 5, 137; b) G. Horowitz, F. Kouki, P. Spearman, D. Fichou, C. Nogues, X. Pan, F. Garnier, *Adv. Mater.* **1996**, 8, 242.
- [10] a) J. Wu, W. Pisula, K. Müllen, *Chem. Rev.* **2007**, 107, 718; b) P. Samorí, V. Francke, K. Müllen, J. P. Rabe, *Chem.-Eur. J.* **1999**, 5, 2312; c) H. Moon, R. Zeis, E. J. Borkent, C. Besnard, A. J. Lovinger, T. Siegrist, C. Kloc, Z. N. Bao, *J. Am. Chem. Soc.* **2004**, 126, 15322.
- [11] F. Würthner, A. Sautter, J. Schilling, *J. Org. Chem.* **2002**, 67, 3037.
- [12] a) R. Li, W. Hu, Y. Liu, D. Zhu, *Acc. Chem. Res.* **2010**, 43, 529; b) Q. Tang, L. Jiang, Y. Tong, H. Li, Y. Liu, Z. Wang, W. Hu, Y. Liu, D. Zhu, *Adv. Mater.* **2008**, 20, 2947; c) Y. Zhang, H. Dong, Q. Tang, S. Ferdous, F. Liu, S. C. B. Mannsfeld, W. Hu, A. L. Briseno, *J. Am. Chem. Soc.* **2010**, 132, 11580.
- [13] a) L. Jiang, J. H. Gao, E. J. Wang, H. X. Li, Z. H. Wang, W. P. Hu, L. Jiang, *Adv. Mater.* **2008**, 20, 2735; b) D. Kumaki, S. Ando, S. Shimono, Y. Yamashita, T. Umeda, S. Tokito, *Appl. Phys. Lett.* **2007**, 90, 053506; c) Q. X. Tang, H. X. Li, Y. L. Liu, W. P. Hu, *J. Am. Chem. Soc.* **2006**, 128, 14634; d) Q. X. Tang, Y. H. Tong, W. P. Hu, Q. Wan, T. Bjørnholm, *Adv. Mater.* **2009**, 21, 4234.
- [14] a) M. Mas-Torrent, M. Durkut, P. Hadley, X. Ribas, C. Rovira, *J. Am. Chem. Soc.* **2004**, 126, 984; b) C. Liu, T. Minari, X. Lu, A. Kumatani, K. Takimiya, K. Tsukagoshi, *Adv. Mater.* **2011**, 23, 523.